JOURNAL OF MAGNETIC RESONANCE **127,** 26–35 (1997)
ARTICLE NO. MN971173

ADRF Differential Cross Polarization Spectroscopy of Synthetic Calcium Phosphates and Bone Mineral

Chandrasekhar Ramanathan*,† and Jerome L. Ackerman*

*Biomaterials Laboratory, NMR Center, Department of Radiology, Massachusetts General Hospital and Harvard Medical School, Charlestown, Massachusetts 02129; and †Division of Health Sciences and Technology and Department of Nuclear Engineering, Massachusetts Institute of Technology, Cambridge, Massachusetts 02139

Received January 30, 1997

An adiabatic demagnetization in the rotating frame (ADRF) differential cross polarization (DCP), or inversion recovery cross polarization (IRCP), technique has been developed to study synthetic calcium phosphates and bone mineral. ADRF of the protons followed by a remagnetization of the phosphorus-31 spins results in an equalization of the dipolar and phosphorus Zeeman nuclear spin temperatures. By shifting the phase of the phosphorus RF by 180° during the forward cross polarization it is possible to invert the temperature of this reservoir and initiate reverse cross polarization. Transient Strombotne–Hahn oscillations were observed on inverting the temperature. The presence of these oscillations complicates the determination of a null point on the basis of cross polarization times. It is necessary to shift the phase of the RF only after a Zeeman spin temperature can be defined, and to use an RF field strength that is slightly smaller than the equivalent S-spin local dipolar field in order to produce a zero crossing after the transient oscillations have decayed.

INTRODUCTION

We are interested in developing *in vivo* solid-state NMR techniques that can provide chemical contrast under conditions of low spectral resolution and low RF power deposition. Our research has been focussed on using NMR to elucidate bone mineral chemistry. Bone mineral is composed primarily of a poorly crystalline nonstoichiometric apatite similar to hydroxyapatite ($Ca_{10}(OH)_2(PO_4)_6$), but also contains HPO_4^{2-} and CO_3^{2-} as well as a variety of cations. For example, it is known that HPO_4^{2-} ion concentrations are the highest in newly deposited bone and that their relative concentration decreases as the mineral matures. Thus the ability to distinguish between PO_4^{3-} and HPO_4^{2-} *in vivo* is of great biochemical interest. Other applications include the study of the resorption and remodeling of calcium phosphate-based bone cements and implants.

The spectral editing technique proposed by Melchior (*1*) is a spectrally selective solid-state technique that has been used to resolve overlapping spectra in heterogeneous, multicomponent polymer systems and organic compounds. It discriminates between species with overlapping spectra on the basis of their cross polarization times and allows selective resonances to be nulled (*2–8*). The technique has been variously called inversion recovery cross polarization (IRCP) (*4*), cross polarization with polarization inversion (CPPI) (*5*), differential cross polarization (DCP) (*6*), and cross polarization–depolarization (CPD) (*7*), in the literature. Wu *et al.* were able to use the DCP technique to suppress the dominant phosphate group and hence detect and identify a unique protonated phosphate present in bone mineral *ex vivo* (*6*).

DCP techniques are usually derived from conventional cross polarization techniques (*9, 10*) and require the simultaneous irradiation of the sample at the resonance frequencies of the two nuclei. Ideally the magnitudes of both these fields should be much larger than the local dipole–dipole fields in the sample. These large fields are difficult to generate over a large volume, as is required when studying macroscopic objects. In addition, large fields are a problem when applied to lossy samples such as biological tissues, as the RF power absorption scales with the square of the RF field amplitude and can produce tissue heating.

This paper describes a DCP technique based on ADRF (adiabatic demagnetization in the rotating frame) cross polarization. ADRF-CP deposits significantly less power when compared to spin-lock CP techniques, and is hence easier to adapt to *in vivo* application. It involves the initial creation of dipolar order via one spin species followed by the transfer of this polarization to the Zeeman system of a second spin species. The ADRF-CP technique was proposed by Anderson *et al.* (*11*) in 1962, but has been used infrequently since then (*12–14*). We have recently described the application of ADRF-CP to the study of calcium phosphates and bone (*15*). These materials are somewhat different from those most often studied with cross polarization as both spin species are comparably abundant.

ADRF CROSS POLARIZATION

Consider a sample containing N_I and N_S spins of two dissimilar spin-$\frac{1}{2}$ systems I and S with gyromagnetic ratios

1090-7807/97 $25.00

γ_I and γ_S, respectively, in an external magnetic field $B_0\hat{k}$. Neglecting the spin–lattice and chemical shift interactions, the spin Hamiltonian of this system is given by (*16*)

$$H = H_I + H_S + H_{DIS}^{RL} + H_{RF}, \quad [1]$$

where

$$H_I = H_{ZI} + H_{DII}^{RL},$$
$$H_S = H_{ZS} + H_{DSS}^{RL},$$
$$H_{RF} = -2\gamma_I B_{1I}\cos(\omega_I t)I_x - 2\gamma_S B_{1S}\cos(\omega_S t)S_x.$$

H_{ZI} is the I-spin Zeeman interaction, H_{DII}^{RL} is the rigid-lattice contribution to the homonuclear I-spin dipolar interaction, H_{ZS} and H_{DSS}^{RL} denote the corresponding S-spin interactions, H_{DIS}^{RL} is the rigid-lattice I–S dipolar interaction, and H_{RF} is the interaction of the applied RF with the spins. Letting $\omega_{0I} = \gamma_I B_0$, $\omega_{0S} = \gamma_S B_0$, $\omega_{1I} = \gamma_I B_{1I}$, and $\omega_{1S} = \gamma_S B_{1S}$, and transforming the resulting Hamiltonian to the tilted rotating frame (TR frame), the Hamiltonian of the spin system can be written as

$$H^\rho = -\omega_{eI} I_{z\rho} - \omega_{eS} S_{z\rho} + H_{DII}^{\rho RL} + H_{DSS}^{\rho RL} + H_{DIS}^{\rho RL}, \quad [2]$$

where

$$\omega_{eI} = \{\omega_{1I}^2 + (\omega_I - \omega_{0I})^2\}^{1/2} \quad [3]$$
$$\omega_{eS} = \{\omega_{1S}^2 + (\omega_S - \omega_{0S})^2\}^{1/2}. \quad [4]$$

The total time-independent dipolar Hamiltonian in the TR frame is derived only from the secular contributions in the laboratory frame. Assuming that the different dipolar terms are strongly coupled to each other, a reasonable assumption given their dense, overlapping spectral distributions (valid for abundant I and S spins), the total dipolar local field in the TR frame is

$$B_{L\rho}^2 = \frac{\mathrm{Tr}\{(H_{DII}^{\rho RL})^2 + (H_{DSS}^{\rho RL})^2 + (H_{DIS}^{\rho RL})^2\}}{\hbar^2\{\gamma_I^2 \mathrm{Tr}(I_{z\rho}^2) + \gamma_S^2 \mathrm{Tr}(S_{z\rho}^2)\}} \quad [5]$$
$$= (B_{LII}^\rho)^2 + (B_{LSS}^\rho)^2 + (B_{LIS}^\rho)^2. \quad [6]$$

In the ADRF cross polarization process the spin system is initially prepared in a state of dipolar order, produced using either an ADRF technique (*11, 17*) or a Jeener–Broekaert pulse pair (*18*). This polarization along the local field can be transferred into an observable Zeeman polarization of the S spins by the application of a resonant RF field. If the S-spin RF field is applied suddenly, there is an initial oscillatory exchange of magnetization between the two spin systems after which thermal mixing takes place between the dipolar and Zeeman reservoirs, and their temperatures equalize. The RF field can also be increased adiabatically from zero so that the two reservoirs are always in equilibrium, their temperatures being equal at all times.

ADRF DIFFERENTIAL CROSS POLARIZATION

Differential cross polarization is performed by instantaneously inverting the temperature of one of the spin systems during the cross polarization process. The sudden disequilibrium and subsequent evolution of the spins toward a common spin temperature may cause the magnetization of the observed spins to pass through zero. The time at which this zero crossing occurs will be different for species with different cross polarization times T_{IS}. As the cross polarization is mediated by the dipolar coupling between the nuclei, the technique is sensitive to the local ordering of the nuclear species. In conventional spin-lock cross polarization the temperature inversion is produced either by applying a hard 180° pulse or, more usually, by shifting the phase of either the I- or S-spin RF by 180°. When this is done rapidly, the ''sudden approximation'' of quantum mechanics applies. The populations of the spin states do not change, but the spins that were spin-locked parallel to the B_1 field will now be spin-locked anti-parallel to the field, resulting in an instantaneous change in the spin temperature of that system from θ to $-\theta$.

As ADRF cross polarization proceeds, the S-spin Zeeman and the dipolar temperatures approach a common value θ_c. If the phase of the S-spin RF is shifted by 180°, the S-spin polarization will now be anti-parallel to the Zeeman field, and the S-spin Zeeman temperature changed instantaneously from θ_S to $-\theta_S$. It should be noted that in the case of ADRF-CP the temperature inversion can only be performed on the S spins as the symmetry between the I- and S-spin systems has been broken. The I spins are aligned along the local dipolar fields and not along an external RF field. The dipolar spin temperature may be inverted with a hard RF pulse, but the efficiency of this approach is poor. An RF pulse of angle α applied to the dipolar system of a sample containing a single-spin species will result in a change in its energy given by (*19*)

$$E_{D\alpha} = E_D(1 - \tfrac{3}{2}\sin^2\alpha), \quad [7]$$

where E_D and $E_{D\alpha}$ are the energies of the dipolar system before and after the pulse. The most negative energy is produced by a $\pi/2$ pulse resulting in a dipolar energy of $-E_D/2$. Thus if θ is the temperature of the system before the pulse, the temperature after the pulse corresponds to a temperature -2θ, which represents a significant loss of polarization. The effect of the pulse becomes more complicated in multiple-spin systems as the transfer efficiency depends on both the homonuclear and heteronuclear dipolar couplings.

If the phase shift is performed after equilibration of the dipolar and Zeeman reservoirs, the spin temperatures of the two systems immediately after the shift are θ_c and $-\theta_c$. Thermal mixing then takes place between the dipolar and Zeeman systems, and the final temperature of the spin system after equilibration θ_f is obtained using the conservation of energy

$$\frac{(C_I + C_S)B_{L\rho}^2 - C_S B_{1S}^2}{\theta_c} = \frac{(C_I + C_S)B_{L\rho}^2 + C_S B_{1S}^2}{\theta_f}, \quad [8]$$

where C_I and C_S are the Curie constants of the I and S spins, respectively. This leads to a final spin temperature

$$\frac{1}{\theta_f} = \left(\frac{(C_I + C_S)B_{L\rho}^2 - C_S B_{1S}^2}{(C_I + C_S)B_{L\rho}^2 + C_S B_{1S}^2}\right)\frac{1}{\theta_c} \quad [9]$$

$$= \left(\frac{F^2 - B_{1S}^2}{F^2 + B_{1S}^2}\right)\frac{1}{\theta_c}, \quad [10]$$

where

$$F^2 = \frac{(C_I + C_S)}{C_S}B_{L\rho}^2 = \left(1 + \frac{C_I}{C_S}\right)B_{L\rho}^2. \quad [11]$$

We call F the equivalent S-spin local field. It is the local magnetic field that the S spins must experience in order to have the same heat capacity as the total secular dipolar reservoir. F is related to ϵ, the ratio of the heat capacity of the S-spin Zeeman reservoir to that of the total dipolar reservoir by $\epsilon = B_{1S}^2/F^2$.

The final observed magnetization after complete equilibration, phased with respect to the magnetization before the temperature inversion, is given by

$$M_f = -\frac{C_S B_{1S}}{\theta_f} \quad [12]$$

$$= \frac{C_S}{\theta_c}B_{1S}\left(\frac{B_{1S}^2 - F^2}{B_{1S}^2 + F^2}\right) \quad [13]$$

$$= M_c\left(\frac{B_{1S}^2 - F^2}{B_{1S}^2 + F^2}\right), \quad [14]$$

where

$$M_c = \frac{C_S B_{1S}}{\theta_c} \quad [15]$$

is the observable magnetization before the phase shift. The ratio of the final magnetization to the magnetization just before the phase shift is

$$R = \frac{M_f}{M_c} = \left(\frac{B_{1S}^2 - F^2}{B_{1S}^2 + F^2}\right). \quad [16]$$

If the temperature inversion is performed after equilibration of the Zeeman and dipolar reservoirs it is possible to produce a zero crossing of the observed magnetization only if the magnitude of the applied RF field is less than the equivalent S-spin local field. When a larger B_{1S} field is applied, it is possible to obtain a zero crossing only if the phase change is performed before the Zeeman and dipolar reservoirs equilibrate. At short times after the phase of the RF is shifted, there is a transient oscillatory exchange of magnetization between the Zeeman and dipolar reservoirs. These Strombotne–Hahn oscillations occur at the effective Larmor frequency ω_{eS} of the S spins in the rotating frame. Transient oscillations observed in regular DCP experiments (*5*) usually occur only in the presence of resolved I–S couplings (*20*), and their frequency depends on the magnitude of the dipolar I–S coupling.

METHODS

Proton to phosphorus DCP experiments were performed on synthetic samples of hydroxyapatite and brushite ($CaHPO_4 \cdot 2H_2O$) (Aldrich Chemical Company, Inc., Milwaukee, WI) as well as a specimen of diaphyseal porcine tibial bone. The specimen of porcine bone was obtained *abattoir*, cleaned of soft tissue, and allowed to dry in air, retaining its complement of protein and lipid. The experiments were conducted in an Omega CSI (formerly General Electric, now Bruker Instruments, Fremont, CA) NMR system equipped with an Oxford Instruments (Oxford, UK) 4.7-T 30-cm horizontal-bore magnet. The proton and phosphorus transmitter frequencies were set on resonance for a sample of phosphoric acid.

A 90° proton pulse followed by a linear ramp demagnetization of the spin-lock field was used to create the dipolar ordered state. The duration of the proton 90° pulses, approximately 65–100 μs, was too long to be considered a hard pulse. However we were limited by the maximum available power and the relatively large sample sizes we are using. The duration of the linear demagnetization ramp used was almost identical to the duration of the 90° pulse. This is effectively a 45° pulse, thus resulting in a Jeener–Broekaert pulse pair rather than a true adiabatic demagnetization of the spins. However, we have found that this sequence results in a reproducible and relatively efficient transfer of Zeeman to dipolar order, given our experimental constraints (*21*).

After a short interval during which both RF fields were off, the phosphorus RF was turned on. An eight-step phase

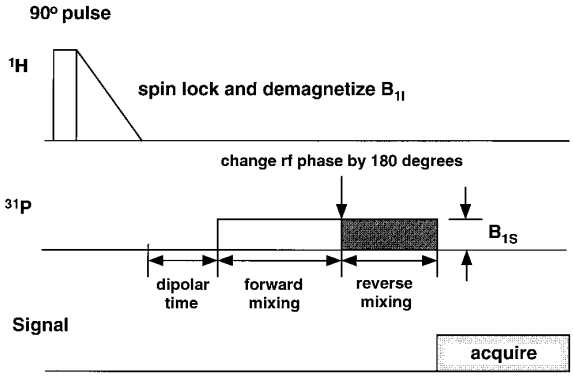

FIG. 1. Pulse sequence for ADRF differential cross polarization using a step RF to remagnetize the phosphorus.

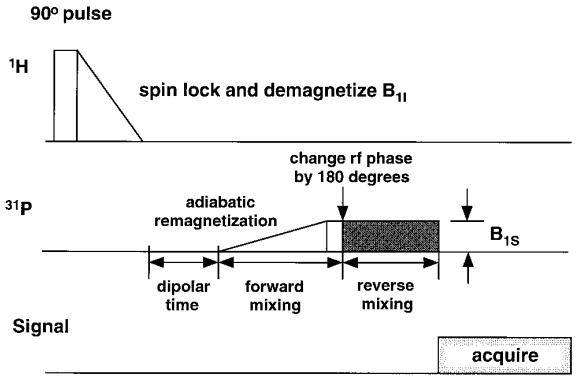

FIG. 2. Pulse sequence for ADRF differential cross polarization using a ramp RF to remagnetize the phosphorus.

cycle, with spin-temperature alternation, was used to remove the nutation signal due to the ^{31}P RF and detect the CP signal. No proton decoupling was used during signal acquisition.

In the first series of experiments the phosphorus RF was suddenly turned on to initiate cross polarization. Differential cross polarization was performed by shifting the phase of the ^{31}P RF by 180° to invert the temperature of the phosphorus spins as illustrated in Fig. 1. Experiments were performed on samples of hydroxyapatite, brushite, and bone under the conditions shown in Table 1. Each spectrum obtained represents a unique combination of forward and reverse cross polarization times.

In the second series of experiments, a slow RF ramp was used to adiabatically remagnetize the phosphorus spins, following the ADRF of the protons. After the remagnetization, the phase of the RF was shifted by 180° and the evolution of the spin system observed. Spectra were collected for varying reverse cross polarization times ranging from zero to 10 ms, and different B_{1S} field strengths. The pulse sequence is shown in Fig. 2 and the experimental parameters are given in Table 2. The experiment was performed on samples of hydroxyapatite and brushite. The duration of the remagnetization ramp was kept fixed at 2 ms for hydroxyapatite and 1.5 ms for brushite.

All the step RF experiments and the hydroxyapatite ramp RF experiment were performed using a two-port double-resonance ^{1}H–^{31}P 4.8-cm diameter single-loop surface coil. A two-port double-resonance ^{1}H–^{31}P 2.5-cm diameter 7.6-cm-long cylindrical resonator was used in the brushite ramp RF experiment.

RESULTS

Each FID was baseline corrected and apodized with a 750-Hz exponential before being Fourier transformed. An isochromat of spins 3 kHz wide centered around the peak was integrated to calculate the signal intensity in the figures illustrating the differential cross polarization. In order to perform the curve fitting to Eq. [16], the spectra were fitted with a Gaussian lineshape, and the peak intensity was recorded. The spectral processing and analysis were performed with the routines of NMR1 (formerly New Methods Research, now Tripos, St. Louis, MO). The curve fitting was performed using the Levenberg–Marquardt method and the Numerical Recipes C programming routines described in Press *et al.* (*22*).

Step RF

In the experiments with the step RF, a number of combinations of forward and reverse cross polarization times were

TABLE 1
Experimental Conditions for Step ADRF-DCP Spectra

	Synthetic calcium phosphates	Bone specimen
Number of acquisitions	64	128
^{1}H 90° pulse	64 μs	64 μs
Demagnetization ramp time	80 μs	80 μs
Dipolar time	300 μs	300 μs
Recycle time	2 s	1.7 s

TABLE 2
Experimental Conditions for Ramp ADRF-DCP Spectra

	Brushite	Hydroxyapatite
Number of acquisitions	64	64
^{1}H 90° pulse	100 μs	64 μs
Demagnetization ramp time	100 μs	80 μs
Dipolar time	100 μs	300 μs
Remagnetization ramp time	1.5 ms	2.0 ms
Duration of constant RF before phase shift	100 μs	500 μs
Recycle time	2 s	2 s

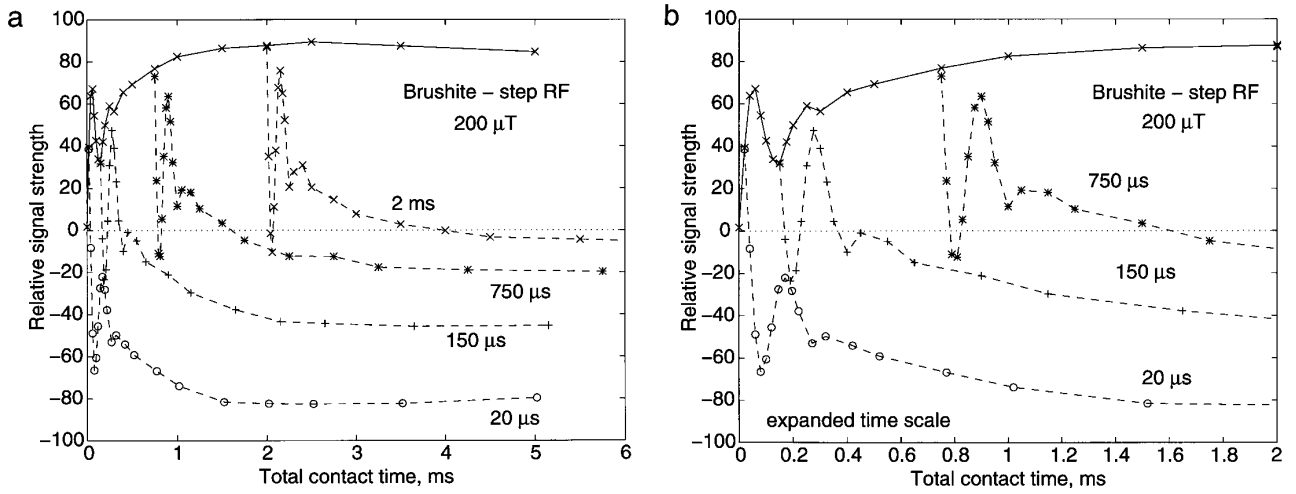

FIG. 3. (a) The effect of inverting the ^{31}P phosphorus temperature at 20 μs, 150 μs, 750 μs, and 2 ms after the initiation of cross polarization in a sample of brushite. The magnitude of the RF field is $\approx$200 μT. The noise level is less than 0.5 units in the figure. (b) The early part of the curve is expanded to show the effect of inverting the phase during the transient oscillation, before the system can be described by a temperature.

used to study the dynamics of the spins under this pulse sequence. The results for brushite are shown in Fig. 3. The usual forward cross polarization signal (solid line) is shown extending out to a contact time of 5 ms. The figure also shows the effect of inverting the ^{31}P phase at 20 μs, 150 μs, 750 μs, and 2 ms after the RF is first turned on. It is observed that the inversion of the signal is stronger if the phase is shifted early in the cross polarization process, before the ^{31}P and ^{1}H can equilibrate completely. Transient oscillations were observed immediately following the phase inversion in every experiment.

At 20 and 150 μs, the transient oscillations due to the sudden application of the RF field have not damped out, and the system cannot be described by a spin temperature. At 750 μs and 2 ms, it appears that the spin temperature description should be valid for this spin system. When the temperature is inverted at 750 μs and 2 ms, the zero crossings are observed to occur after the new transient oscillations have decayed, at approximately 1.6 and 4 ms of total contact time, respectively, and should be determined only by the cross polarization times. When the temperature was inverted at 2 ms, the asymptotic value of the curve was small and negative, indicating that magnitude of the B_{1S} field ($\approx$200 μT) is slightly smaller than the magnitude of the equivalent S-spin local field as described by Eq. [16].

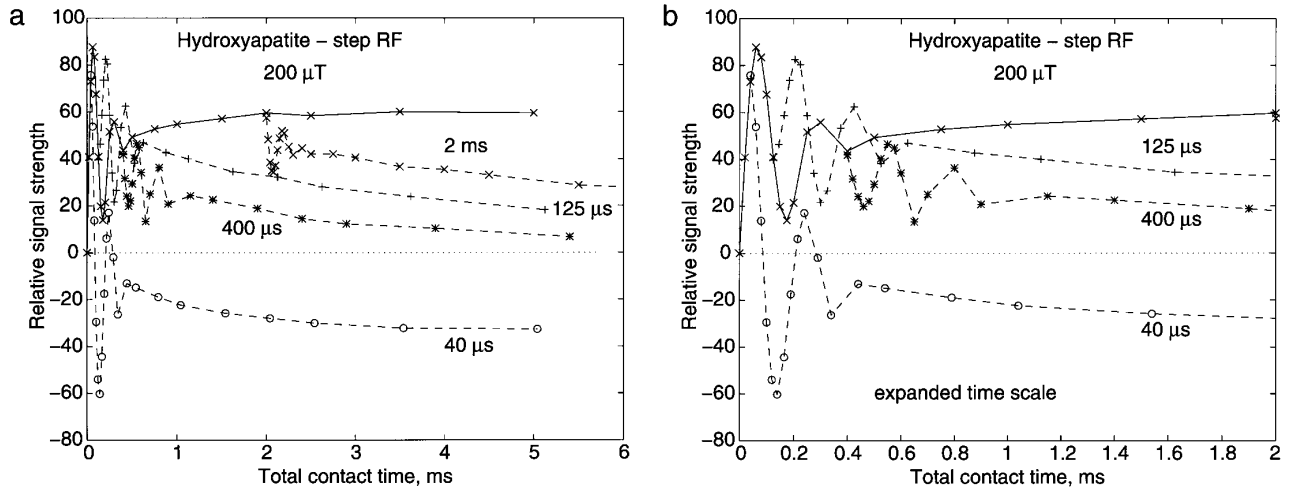

FIG. 4. (a) The effect of inverting the ^{31}P phosphorus temperature at 40 μs, 125 μs, 400 μs, and 2 ms after the initiation of cross polarization in a sample of hydroxyapatite. The magnitude of the RF field is $\approx$200 μT. The noise level is less than 0.35 units in the figure. (b) The early part of the curve is expanded to show the effect of inverting the phase during the transient oscillation, before the system can be described by a temperature.

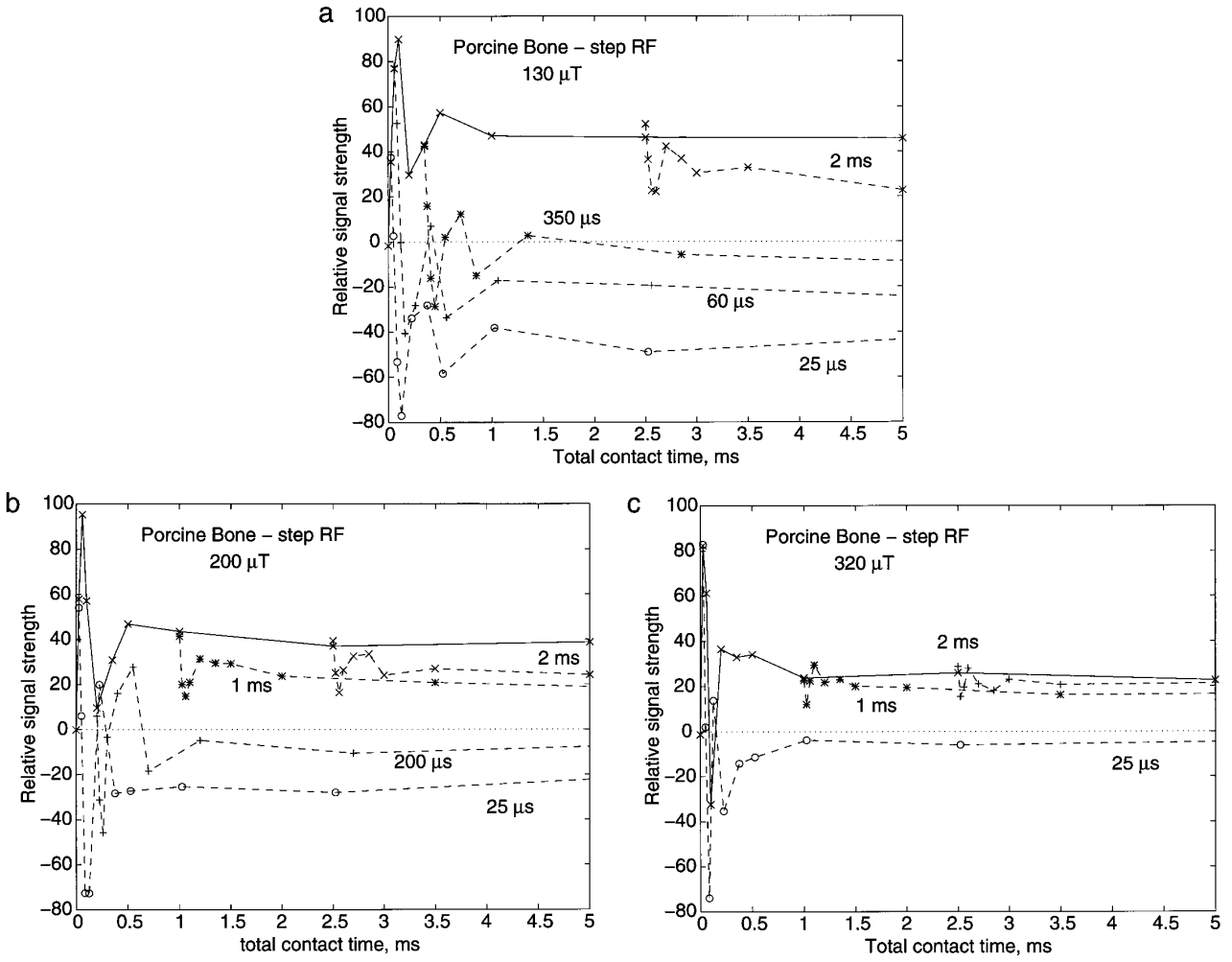

FIG. 5. The effect of inverting the ^{31}P phosphorus temperature at various times during the cross polarization process in the bone specimen. The three RF field strengths are (a) 130 μT, (b) 200 μT, and (c) 320 μT. The noise level is less than 0.8 units in the scale displayed.

The response of the hydroxyapatite spin system to the step RF experiment is illustrated in Fig. 4. It shows the effect of inverting the temperature at 40 μs, 125 μs, 400 μs, and 2 ms after the RF is first turned on. Once again the inversion of the signal is stronger if the phase is shifted early in the cross polarization process before equilibration proceeds very far. The signal was observed to pass through zero only if the phase was shifted during the early part of the transient oscillation, indicating that the value of the B_{1S} field ($\approx$200 μT) is greater than that of the equivalent S-spin local field. The slope of the oscillation immediately after the inversion of the phase is the negative of the slope just before the inversion, as can be seen in Fig. 4b.

The response of the bone specimen to the step RF field is shown in Fig. 5 for three different field intensities of 130, 200, and 320 μT. The strongest cross polarization takes place at the lowest field. The response of the ^{31}P spins to the temperature inversion is also the greatest in the 130-μT field, indicating strong thermal contact between the two systems. However, even the 130-μT field is larger than the equivalent S-spin local field of the bone specimen. At 320 μT there was a very small response to the phase change after the initial oscillation.

Figure 6 shows the series of spectra obtained when the phase is inverted 60 μs after the RF is turned on. There is a strong oscillation before the asymptotic signal can be observed. Note the change in shape of the spectra at 1, 2.5, and 5 ms. The linewidths obtained from a Gaussian curve fitted to the spectra at these times are 4450, 3400, and 3000 Hz respectively. This is expected as the broader protonated spectral components cross polarize faster than the nonprotonated components, and hence invert faster. The broad spectrum at a 1-ms reverse cross polarization time is indicative of the presence of HPO_4^{2-} groups in the bone. Figure 7 allows direct comparison of the spectra just before the phase shift (lw = 2300 Hz) and after 1 ms of reverse cross polarization (lw = 4450 Hz).

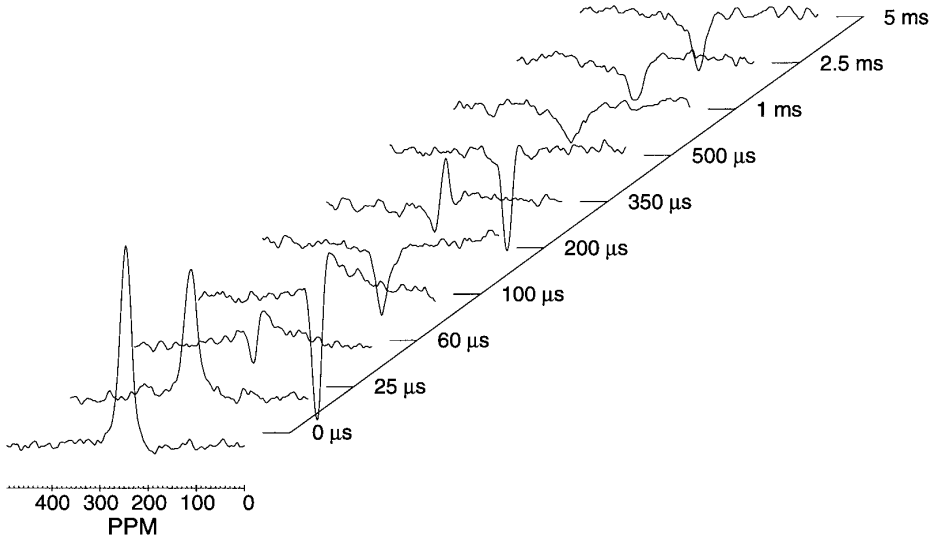

FIG. 6. The spectra of porcine bone obtained at different reverse cross polarization times—indicated in the figure—after a forward cross polarization time of 60 μs. The RF field strength is 130 μT.

Ramp RF

In these experiments a linear ramp remagnetization was performed on the phosphorus spins to different maximum RF field strengths. After a brief interval during which the RF was kept constant, the RF phase was shifted by 180° while the magnitude was kept fixed.

The results obtained with brushite are shown in Fig. 8 for B_{1S} field strengths of 63, 260, 385, and 430 μT. The 63-μT curve is seen to invert rapidly, while the 260-μT curve inverts much more slowly, at approximately 1.8–2 ms contact time, after the initial oscillations have decayed. The 385- and 430-μT curves do not change significantly after a large initial transient oscillation. The transient oscillations are observed in all cases.

The results of the ramp remagnetization experiment on hydroxyapatite are shown in Fig. 9, and closely parallel those of brushite. For B_{1S} = 73 μT there is a strong response to the change in the RF phase. The cross polarization rate is comparatively the fastest at this field, and the magnetization is seen to slowly invert at approximately 6 ms of reverse cross polarization time. The 130- and 220-μT curves indicate some contact between the dipolar field and the Zeeman field with slower cross polarization times, while the 515- and 630-μT fields indicate almost no contact

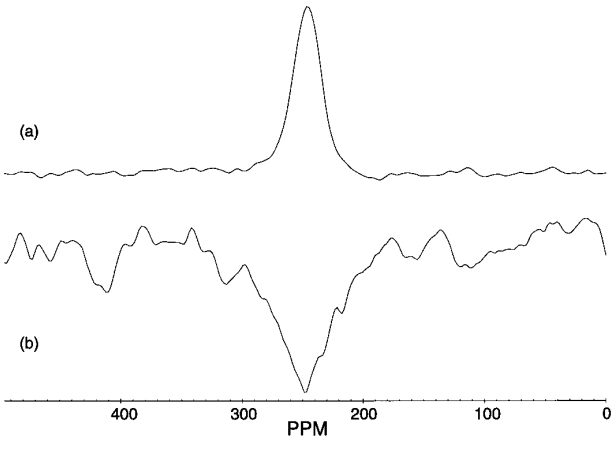

FIG. 7. The spectrum of porcine bone obtained at (a) a forward cross polarization time of 60 μs, and (b) after an additional 1 ms reverse cross polarization. The linewidth of the best Gaussian fit is 2300 Hz for spectrum (a) and 4450 Hz for spectrum (b). The RF field strength is 130 μT.

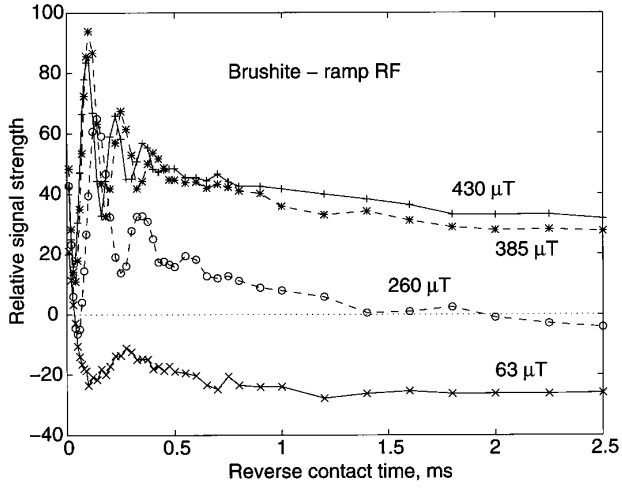

FIG. 8. The effect of inverting the phase after an adiabatic remagnetization of the ^{31}P spins of brushite to maximum fields of 63, 260, 385, and 430 μT. The noise level is less than 0.5 units in the displayed scale.

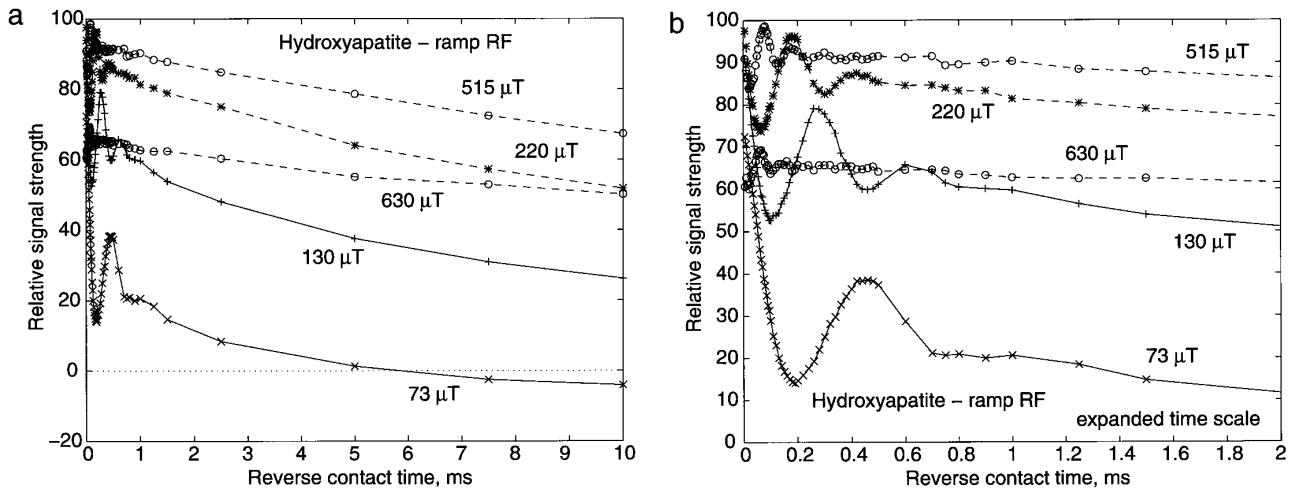

FIG. 9. (a) The effect of inverting the phase after an adiabatic remagnetization of the ^{31}P spins of hydroxyapatite to maximum fields of 73, 130, 220, 515, and 630 μT. The noise level is less than 0.2 units in the displayed scale. Note the change in the cross polarization rate with the magnitude of the B_{1S} field. (b) The early part of the curve is shown expanded in time to illustrate the transient response of the system.

between the two systems. Note that the amplitude of the transient oscillation also decreases as the B_{1S} field strength is increased. The small initial value of the 630-μT curve is due to the nonadiabaticity of the ramp remagnetization to this field. A slower ramp is needed in this case to achieve an adiabatic remagnetization.

The ratio of the final magnetization after 5 ms of reverse cross polarization to that when the phase is changed is plotted as a function of B_{1S} field strength in Figs. 10 and 11. The points have been fitted to the expected functional form of Eq. [16] using F as the only adjustable parameter. The best fits to the brushite and hydroxyapatite data yield equivalent S-spin local fields of 256 ± 13 and 89 ± 3 μT, respectively.

DISCUSSION

Spectral Editing

The sudden disequilibrium between the ^{1}H and ^{31}P spins produced transient Strombotne–Hahn oscillations in all our experiments. These oscillations occur at the effective Larmor frequency ω_{eS} of the ^{31}P spins, and therefore depend on the

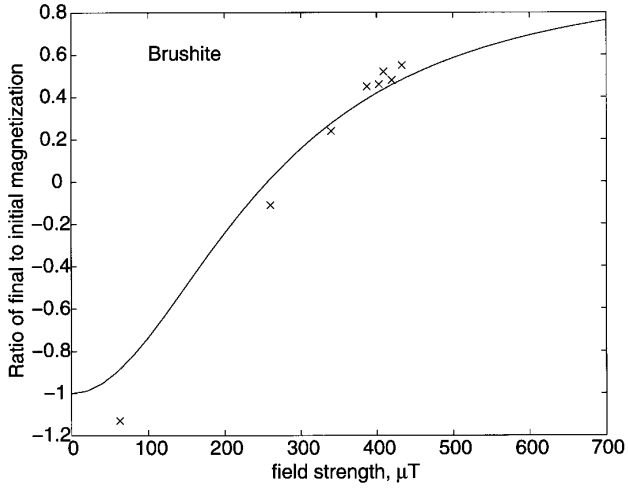

FIG. 10. The ratio of the final magnetization (after 5 ms of reverse cross polarization) to the initial magnetization (at the start of the reverse cross polarization) as a function of RF field strength for brushite. The smooth curve is the best fit of Eq. [16] to the data points, yielding an equivalent S-spin local field value of 256 ± 13 μT.

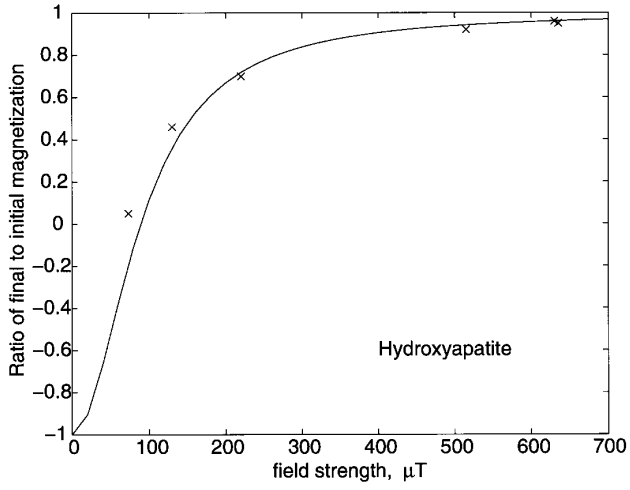

FIG. 11. The ratio of the final magnetization (after 5 ms of reverse cross polarization) to the initial magnetization (at the start of the reverse cross polarization) as a function of RF field strength for hydroxyapatite. The smooth curve is the best fit of Eq. [16] to the data points, yielding an equivalent S-spin local field value of 89 ± 3 μT.

amplitude of the RF field applied. The presence of these transient oscillations makes it complicated to predict the zero crossing of the signal based on the cross polarization time T_{IS} alone, as is usually done in conventional DCP experiments.

In the step RF case, only the brushite spectra in which the phase reversal was performed at 750 μs and 2 ms produced zero crossings after the initial transient oscillations had decayed. In the ramp remagnetization study, the 73-μT hydroxyapatite spectrum was observed to slowly invert at about 6 ms, and the 260-μT brushite spectrum was observed to invert at about 1.8–2 ms. In the case of the adiabatic remagnetization, the magnitude of the RF field should be smaller than the equivalent S-spin local field; otherwise, no zero crossing will be observed as described by Eq. [16]. If the magnitude of the RF field is too small there is no clear zero crossing as the magnetization remains negative after the oscillations have damped out. It is necessary to choose the amplitude of the RF field to be smaller than the equivalent S-spin local field, yet sufficiently large so as to ensure that the cross polarization time T_{IS}, which is also dependent on the RF field strength (*13*), is long enough that the zero crossing occurs after the oscillations have decayed. In the case of the step RF field, the phase change should be performed only after the initial oscillations have decayed, and the phosphorus spins can be described by a spin temperature.

It is interesting to note from Eq. [16] that it should also be possible to suppress one component of a multicomponent system by using an RF field whose magnitude is equal to the equivalent S-spin local field of the component to be suppressed ($B_{1S} = F$).

Spin Calorimetry

As long as the experiments are conducted in a time short compared to the spin–lattice relaxation times T_{1D} and $T_{1\rho}$ of the sample, it is possible to perform simple calorimetry with the two spin systems. In addition, as the heat capacity of the ^{31}P spins depends on the magnitude of the RF field, it is also possible to find the strength of the equivalent S-spin local dipolar field of the sample. We obtained equivalent S-spin local field values of 256 $\pm$ 13 μT for brushite and 89 $\pm$ 3 μT for hydroxyapatite. Incomplete equilibration of the spin systems before and after the temperature inversion as well as $T_{1\rho}$ effects have been neglected in the current model. Incorporating these considerations could improve the theoretical fit to the data, although it will lead to the introduction of a number of additional parameters. It should also be possible to combine the results of these experiments with those of proton-observe experiments to calculate the effective ratio of the Curie constants of the two spins, indicating the number of proton spins in effective dipolar contact with each phosphorus spin.

The ramp remagnetization experiments show that it is possible to effectively break thermal contact between the Zeeman and dipolar reservoirs by increasing the strength of the RF sufficiently. By varying the size of the applied RF field the interaction of these reservoirs can be examined over different regimes.

CONCLUSIONS

We have presented an ADRF-CP variant of the DCP technique. The presence of transient oscillations made it difficult to select a specific set of forward and reverse cross polarization times to achieve spectral selection based on T_{IS} differences. It is necessary to carefully select the magnitude of the RF field used, as well as the time at which the ^{31}P spin temperature is inverted in order to be able to perform spectral selection. However, it should be possible to find an appropriate set of parameters in order to achieve a particular selectivity, if the values of T_{IS} and the various T_1 times are sufficiently different from each other. Alternately, the ADRF DCP technique can also be used to provide spectral selection on the basis of the equivalent S-spin local field. It was possible to perform spin calorimetry experiments and obtain the value of the equivalent S-spin local fields of brushite and hydroxyapatite.

ACKNOWLEDGMENTS

This work was funded in part by National Institutes of Health Grant AR42258 from the National Institute of Arthritis and Musculoskeletal and Skin Diseases. C.R. acknowledges support from a predoctoral award from the Massachusetts General Hospital Fund for Medical Discovery. We thank Dr. Yaotang Wu of Children's Hospital in Boston, for providing us with some of the curve fitting routines used in this paper. We also thank Professor D. G. Cory of MIT for several helpful suggestions.

REFERENCES

1. M. Melchior, Abstracts of the 22nd Annual Experimental NMR Conference, Pacific Grove, CA (1981).
2. N. Zumbulyadis, *J. Chem. Phys.* **86,** 1162–1166 (1987).
3. X. Wu, S. Zhang, and X. Wu, *J. Magn. Reson.* **77,** 343–347 (1988).
4. D. G. Cory and W. M. Ritchey, *Macromolecules* **22,** 1611–1615 (1989).
5. X. Wu and K. Zilm, *J. Magn. Reson. A,* **102,** 205–213 (1993).
6. Y. Wu, M. J. Glimcher, C. Rey, and J. L. Ackerman, *J. Mol. Biol.* **244,** 423–435 (1994).
7. R. Sangill, N. Rastrup-Andersen, H. Bildsoe, H. J. Jakobsen, and N. C. Nielsen, *J. Magn. Reson. A* **107,** 67–78 (1994).
8. C. Bonhomme, F., Babonneau, J. Maquet, J. Livage, M. Vaultier, and E. Framery, *J. Chim. Phys.* **92,** 1881–1884 (1995).
9. A. Pines, M. G. Gibby, and J. S. Waugh, *J. Chem. Phys.* **56,** 1776–1777 (1972).
10. A. Pines, M. G. Gibby, and J. S. Waugh, *J. Chem. Phys.* **59,** 569–590 (1973).
11. A. G. Anderson and S. R. Hartmann, *Phys. Rev.* **128,** 2023–2041 (1962).
12. F. M. Lurie and C. P. Slichter, *Phys. Rev.* **133,** A1108–A1122 (1964).

13. D. A. McArthur, E. L. Hahn, and R. E. Walstedt, *Phys. Rev.* **188,** 609–638 (1969).

14. J. L. Ackerman, J. Tegenfeldt, and J. S. Waugh, *J. Am. Chem. Soc.* **96,** 6843–6845 (1974).

15. C. Ramanathan, Y. Wu, B. Pfleiderer, M. J. Lizak, L. Garrido, and J. L. Ackerman, *J. Magn. Reson. A* **121,** 127–138 (1996).

16. D. Wolf, ''Spin-Temperature and Nuclear-Spin Relaxation in Matter: Basic Principles and Applications,'' Clarendon Press, Oxford (1979).

17. C. P. Slichter and W. C. Holton, *Phys. Rev.* **122,** 1701–1708 (1961).

18. J. Jeener and P. Broekaert, *Phys. Rev.* **157,** 232–240 (1967).

19. J. Jeener, H. Eisendrath, and R. Van Steewinkel, *Phys. Rev.* **133,** A478–A490 (1964).

20. L. Müller, A. Kumar, T. Baumann, and R. R. Ernst, *Phys. Rev. Lett.* **32,** 1402–1406 (1974).

21. C. Ramanathan and J. L. Ackerman, Abstracts of the 37th Annual Experimental NMR Conference, March 17–22, Pacific Grove, CA (1996).

22. W. H. Press, S. A. Teukolsky, W. T. Vetterling, and B. P. Flannery, ''Numerical Recipes in C,'' second ed., Cambridge Univ. Press, Cambridge, UK (1992).